Received: 28 October 2023 | Revised: 7 March 2024 | Accepted: 12 March 2024

DOI: 10.1111/sum.13052

Soil Use and Management | WILEY

RESEARCH ARTICLE

Enhancing soil properties through sustainable agronomic practices reduced the occurrence of kiwifruit vine decline syndrome

Adriano Sofo[1] | **Bartolomeo Dichio**[1] | **Hazem S. Elshafie**[2] | **Ippolito Camele**[2] | **Maria Calabritto**[1] | **Isabella Tomasi**[3] | **Marco Mastroleo**[4] | **Evangelos Xylogiannis**[4] | **Ilaria D'Ippolito**[1,5] | **Alba N. Mininni**[1]

[1]Department of European and Mediterranean Cultures (DiCEM), Università Degli Studi Della Basilicata, Matera, Italy

[2]School of Agriculture, Forest, Food and Environmental Sciences (SAFE), Università Degli Studi Della Basilicata, Potenza, Italy

[3]Vitaceres SAS Consultante, Codognan, France

[4]Zespri Innovation Ltd, Mt. Manganui South, New Zealand

[5]Mediterranean Agronomic Institute (CIHEAM), Valenzano, Italy

Correspondence
Adriano Sofo, Department of European and Mediterranean Cultures: Architecture, Environment and Cultural Heritage (DiCEM), Università degli Studi della Basilicata, Via Lanera 20, 75100 Matera, Italy.
Email: adriano.sofo@unibas.it

Funding information
Zespri International Ltd

Abstract

Kiwifruit vine decline syndrome (KVDS) is an emerging challenge related to various factors, including water stagnation, soil compaction, root hypoxia, imbalanced soil redox potential, soil nutrient imbalance and fungal pathogens, yet its definitive causes remain unconfirmed. This study compared soils and roots of healthy plants (CTRL group) and plants affected by KVDS (KVDS group) at a kiwifruit orchard (*Actinidia chinensis* cv. '*Zesy002*') in Sermoneta (Lazio region), Italy. Our findings indicate that soil redox potential, a parameter related to soil oxidation, and soil macroporosity were significantly lower in the KVDS soils. The water table was also found to be higher in the KVDS block of the orchard, demonstrating a higher soil water content. This suggests less aeration and more water content in KVDS-affected soils compared to the control. Root analyses showed that KVDS led to browning and decomposition of rhizodermis, decay of the central stele, detachment of the cortex, reduced cell size and the presence of starch granules in the parenchyma, with significant variations in root morphometric parameters. To mitigate KVDS, sustainable agronomic practices, including precision irrigation, green manure, compost addition and water drainage root pruning, were carried out on some KVDS-symptomatic vines (SUST group). Molecular analyses revealed the presence of 10 fungal species from treated root plants, with *Paraphaeosphaeria michotii*, *Fusarium oxysporum* and *Ilyonectria vredenhoekensis* being frequently isolated from symptomatic KVDS-affected plants but less from SUST plants. Also, *Beauveria bassiana* and *Bacillus amyloliquefaciens*, showed an effect against *I. vredenhoekensis* and *P. michotii*, and may be suitable candidates as biocontrol agents. The adoption of sustainable agronomic practices resulted in significantly more healthy plants (46% increase) by the end of the trial, demonstrating that a sustainable soil use and water management at kiwifruit orchards can mitigate KVDS through restoration of natural growth conditions.

KEYWORDS

green manure, root microscopy, soil macroporosity, sustainable soil management, waterlogging

1 | INTRODUCTION

Kiwifruit has been a growing part of the Italian fruit growing sector since 1970 (Donati et al., 2020; Savian, Martini, et al., 2020). However, the industry is threatened by the emergence and progressive spread of 'kiwifruit vine decline syndrome' (KVDS) (Bardi, 2020; Manici et al., 2022), resulting in a ~30% decrease in Italian total kiwifruit production (Donati et al., 2020).

The causes are not fully known, but recent findings suggest improper agronomic and irrigation management practices bring about KVDS through waterlogging, soil compaction, root hypoxia, imbalance of soil nutrients and the concomitant action of phytopathogens, whose synergic action causes the decline of the plants (Savian, Ginaldi, et al., 2020; Sofo et al., 2022). Other studies point to a possible co-role of changing climatic conditions, particularly high atmospheric temperature, as triggering factors of KVDS (Bardi, 2020; Bardi et al., 2020). Report of KVDS in northern Italy was first made in 2012 (Donati et al., 2020), but manifestations of KVDS-like symptoms, including the appearance of large necrotic areas on the leaves were first reported in New Zealand in 1989 by Smith et al. (1989) and later confirmed by Reid et al. (1991), who attributed the condition to poor soil oxygenation and to the sensitivity of kiwifruit roots to hypoxic soil conditions.

Foliar symptoms of KVDS, such as epinasty, chlorosis, desiccation and abscission, are a consequence of a low root/canopy ratio because of the damage to kiwifruit root systems, in terms of reduced development, tissue breakdown and decomposition, anomalous anatomy structure and presence of necrotic areas (Bardi et al., 2020; Sofo et al., 2022). Therefore, soil mismanagement together with poor irrigation management, leading to a compacted, impermeable and hypoxic soil layer, is thought to be a major cause of kiwifruit root disruption and KVDS emergence (Bardi, 2020; Savian, Ginaldi, et al., 2020; Sofo et al., 2022).

On the other hand, the role of soil microorganisms cannot be overlooked as a cause (or consequence) of KVDS. Since 2008, the kiwifruit sector has suffered bacterial canker of kiwifruit, whose etiological agent is *Pseudomonas syringae* pv. *actinidiae* (Donati et al., 2014). Recently, it was found that potential fungal pathogens isolated from KVDS-symptomatic plants may play a role in inducing the KVDS in potted plants (Donati et al., 2020; Savian et al., 2021; Savian, Ginaldi, et al., 2020; Spigaglia et al., 2020). However, the role of these microorganisms in field conditions remains unclear. Savian, Ginaldi, et al. (2020); Savian et al. (2021) used a metabarcoding approach to detect putative *Phytopythium* spp. pathogens associated with KVDS but, at the same time, the role of synergic and cumulative effects of biotic and abiotic agents in KVDS emergence was highlighted.

There is increasing evidence to support the importance of reduction–oxidation (redox potential, Eh) and acid–base reactions in the soil–plant system (Husson et al., 2021). Roots thrive within a specific Eh-pH spectrum and rely on various processes to ensure their homeostasis, which plays a central role in plant health (Husson et al., 2018). The Eh-pH conditions in the soil rhizosphere result from multiple interactions between soil physicochemical components, soil microbiota and plant roots (Husson et al., 2016). Our hypothesis is that soil resilience against potential fungal pathogens of kiwifruit plants could derive, in-part, from good soil structure and aeration, leading to diverse Eh-pH niches that harbour a diversity of antagonists through aggregates with more aerobic environments.

Considering the crucial role of soil in mitigating or avoiding the progression of KVDS and elucidating the eventual role of soil biological fertility and soil microorganisms, a series of sustainable agronomic field experiments should be carried out on KVDS-symptomatic vines. On this basis, we considered precision irrigation, organic matter addition and cover crops sowing. The objectives were to: (i) assess microscopically the root damage occurring in KVDS-symptomatic plants; (ii) evaluate the values of Eh-pH and macroporosity of soils where grew plants with and without KVDS symptoms; (iii) isolate, identify and determine the frequency of the fungal species associated with KVDS in response to different agronomic managements; (iv) assessing the effectiveness of two antagonist microorganisms against the three dominant pathogenic fungi isolated from plants with KVDS and (v) evaluate the overall plant physiological status by a visual scoring method.

2 | MATERIALS AND METHODS

2.1 | Experimental site and orchard management

The experimental kiwifruit orchard, located in Sermoneta (Lazio region), Italy (41°33′30.72″ N; 12°57′18.51″ E), is characterized by an average (2020–2022) annual ET_o of 962 mm and annual rainfall of 895 mm, with an average environmental water deficit during the irrigation season (April–September) of 440 mm. Conventionally for the area, the applied irrigation volumes were approx. 6500–7000 $m^3\,ha^{-1}\,year^{-1}$, exacerbating water excess conditions. The cultivated variety was *Actinidia chinensis* (Planch.) var. *chinensis* cv. '*Zesy002*', a yellow-fleshed kiwifruit, grafted onto Hayward rootstocks (*Actinidia chinensis* var. *deliciosa*) in 2013. Planting was conducted 5 × 3 m on inter-row and row, respectively, for a total 666 plants ha^{-1}.

For control (CTRL) and KVDS plants, the irrigation system is composed one drip line and sprinkler system both located in the row. The irrigation was empirically managed (average annual irrigation volume of about 6500–7000 $m^3\,ha^{-1}\,year^{-1}$). For sustainable practices (SUST) plants, the irrigation system was changed introducing two independent drip lines at about 50 cm from the trunk and the sprinkler system with one sprinkler at 60 $L\,h^{-1}$ per tree. The precision irrigation strategy was based on the water-balance method with a feedback adjustment mechanism using continuous soil moisture measurements was applied (Mininni et al., 2022). The irrigation strategy allowed us to adapt irrigation volume (average of 4500 $m^3\,ha^{-1}\,year^{-1}$) to actual vine water requirement and ensure optimal soil conditions for root development, avoiding the establishment of conditions predisposing degenerative phenomena of the root system.

A 3-year experimental trial commenced in February 2020. The soil was supplemented with mineral fertilizers in April–September 2020 (100 units N ha^{-1}, 120 units K ha^{-1}, 90 units Ca ha^{-1} and 30 units Mg ha^{-1}) and a foliar application of phytohormones and NPK fertilizer (Spray Dünger® Global; Biolchim SpA, Medicina, Bologna, Italy) at a rate of 5 kg ha^{-1} plus 5 units Ca ha^{-1}. In 2021, the SUST group was fertilized with organic soil conditioners (manure and compost) with no mineral fertilizers, while the CTRL and KVDS groups had fertilizers applied as in 2020. Soil physicochemical parameters measured in February 2021 are reported in Table S1.

At the beginning of the experiment (February 2020), an area of the orchard site with vines showing severe visual symptoms of KVDS (KVDS group), and another with healthy plants (CTRL group) were identified (Figure S1). The severe KVDS symptoms included phylloptosis, shoot wilting, fruit size reduction and heavy aesthetic defects that make the fruits unmarketable.

Starting from the second year of the experiment (2021), a set of agronomic practices was carried out on some KVDS-symptomatic vines (KVDS group) in order to mitigate/avoid the progression of the KVDS. This included precision irrigation, sowing of specific cover crops, the addition of manure and water drainage. In addition, root pruning was performed to promote the formation and development of new roots in the soil interested in the abovementioned sustainable practices (SUST group). Root pruning took place in March 2021 by deep vertical cutting of the roots at a distance of ~70 cm from the trunk on the four sides of the plant (Figure S2). In SUST plants, two green manure cycles (150 kg seeds ha^{-1}, distributed with a manual seeder) were applied between March 2021 (sowing) and June 2021 (moving), and between December 2021 (sowing) and April 2022 (moving) (Figure S3). The cover crop mixture (MAS Seeds Italia Srl, San Pietro di Morubio, Verona, Italy) is shown in Table S2. Immediately after green manure sowing, mature manure was distributed on the row, close to the plants, with a manure spreader at an amount of 80 q ha^{-1}. The chemical composition of manure is reported in Table S3.

To increase soil aeration and decrease hypoxia in the orchard, a drain (10 cm diameter) was positioned in the middle of the row, each of two rows, at a depth of 90 cm (Figure S4). The installation of drainage followed water table monitoring with piezometers since the beginning of 2021. Three piezometer couples were installed in the orchard (Figure S5): the piezometers (called '1, 2, 3' in the figure) were 10 m spaced on the row and 150 cm deep. Each piezometer had a replica (called '1B, 2B, 3B') close to the tractor pneumatic path, to explore water lateral movements. Another spare piezometer (C) (80 cm deep) was installed on the row, to examine irrigation water movement.

Finally, in one SUST plant, an excavation was made on three sides, one on the row (perpendicular to the row) and two toward the inter-row (parallel to the row), in order to add peat all around (SUST-PE). The addition of peat was done to allow the root system to fully express its regeneration potential, contributing to understand the capacity of formation and development of viable and stronger roots, capable of recovering from KVDS symptoms.

2.2 | Root microscopy

In February 2022, fine root samples were collected at a depth of 30–40 cm from three healthy control plants (CTRL) and three KVDS-affected plants (KVDS). The soil was manually excavated at a distance of ~70 cm from the trunk, and fine roots (diameter < 5 mm) were cut, lightly washed with tap water and immediately fixed in 10% (v/v) formalin to preserve the morphology and chemical composition of the tissues. In the laboratory, roots were dehydrated to an alcohol scale to replace the tissue water with a miscible agent, with the cleared paraffin solvents for impregnating tissues with a paraffin solvent and embedded in paraffin. Each individual sample was sectioned with a rotating microtome into sections with a thickness of 5 µm and stained with safranin-fast green or PAS-emallume, according to Ma et al. (Ma et al., 2011) and Albrecht and Mustroph (2003) respectively. The sections were observed by a light microscope (Nikon Eclipse E600; Tokyo, Japan), and photographed with a digital camera (Nikon DXM1200). After that, root morphometric parameters (root diameter, total root area, rhizodermis thickness, parenchymatic cell size, cortex thickness, cortex area, central stele diameter, central stele area, central stele area/cortex area) were measured using ImageJ software (https://

imagej.nih.gov/ij/) on 20 measurements taken from each of the three plants per group ($n = 60$).

2.3 | Measurement of soil redox potential and soil macroporosity

In February 2021, nine soil samples were taken (in triplicate) with an auger at depths of 0–30, 30–60 and 60–90 cm, placed in plastic bags and immediately used for the following analyses. For the topsoil (0–30 cm), vegetation and its eventual residues were removed manually before sampling the soil. Soil redox potential was measured by potentiometric determination using a 1:2.5 suspension from ground to liquid phase ratio and reading after 5 h with an Orion Star A214 voltmeter (Fisher Scientific, Waltham, MA, USA), and a metallic combination electrode with the reference Ag/AgCl (KCl 3 M) Thermo Scientific Orion (Fisher Scientific). The E value for each sample was the E (in mV), indicated on the voltmeter that was associated after 1 min with no change in the E unit. After being measured, according to the Ag/AgCl reference electrode, all potentials versus Ag/AgCl were transformed to give the values of redox potentials (Eh) according to the normal hydrogen electrode (NHE) with the relationship between the Ag/AgCl reference, temperature and NHE provided by the instrument. Soil pH was measured according to Pansu and Gautheyrou (2006) with a glass electrode (model Basic 20; Crison Instruments SA, Barcelona, Spain) in distilled water, using a 1:2.5 suspension from ground-to-liquid phase ratio.

In order to better define the redox conditions of the soils studied, Eh was adjusted to pH = 7 (Husson et al., 2016):

$$\mathrm{Eh_{pH7}} = \mathrm{Eh} - \frac{\mathrm{RT}}{\mathrm{F}} \times \ln 10 \times (7 - \mathrm{pH}), \quad (1)$$

where $\mathrm{Eh_{pH7}}$ is the soil redox potential at pH = 7, R is the perfect gas constant (8.314 J K^{-1} mol^{-1}), T is the temperature in Kelvin (25°C = 298°K) and F is the Faraday constant (96,485 C mol^{-1} = 1 F).

On the same soil samples, soil macroporosity was determined using a transmitted light microscopy (model ADL 601 P 40-600x; Bresser GmbH, Rhede, Germany) connected to a digital camera (model MikroCam II 20 MP 1″; Bresser GmbH, Rhede, Germany). Soil thin sections (30 μm) embedded in epoxy resin (Durcupan™; Sigma-Aldrich, St. Louis, MI, USA) (Figure S6) were prepared following the method of Sotta and Fujiwara (Sotta & Fujiwara, 2017) and percentage total macropore volume was evaluated by Image J software (https://imagej.nih.gov/ij/index.html). Three soil sections from each of the three soil replicates were obtained and the values of macroporosity averaged ($n = 27$).

2.4 | Fungal isolation and identification

In February 2022, a mechanical excavator was used or create trenches in the inter-row area at a depth of about 90 cm and at a distance of about 70 cm from the trunk of plants belonging to the four groups (CTRL, KVDS, SUST and SUST-PE) (Figure S7). In this circumstance, fine roots (diameter <5 mm) taken from all groups at a depth of 30–40 cm (where kiwifruit roots are denser; Bardi, 2020; Bardi et al., 2020) were placed on Petri dishes containing potato dextrose agar (PDA) nutrient media, pre-supplemented with ampicillin and kanamycin (Sigma-Aldrich, St. Louis, MO, USA) and incubated at 24°C until visible colony formation. In particular, for CTRL, KVDS, SUST and SUST-PE, 56, 84, 63 and 45 root samples, taken from three plants for each group, were analysed respectively. The grown fungi were purified, and morphologically and molecularly identified. The total number of the fungal isolates for each group category were counted and the fungal frequency percentage (FFP) was calculated as follows:

$$\mathrm{FFP}\,(\%) = \frac{\text{Number of each isolated fungal species}}{\text{Total number of isolated fungal species}} \times 100. \quad (2)$$

The identification of the pure fungal colonies was carried out based on morphological features using an optical microscope (Zeiss Axioskop model; Oberkochen, Germany) connected to a digital camera. In addition, a precise identification has been carried out based on molecular methods. For this scope, fresh fungal culture (100 mg) was used for extraction of the total genomic DNA (gDNA) using the DNeasy Plant Mini Kit (Qiagen; Heidelberg, Germany) following manufacturer's instructions. The extracted gDNA was quantified and purity-analysed using Nanodrop (ND-1000 spectrophotometer; Thermoscientific Inc., Whatman, MA, USA) and conserved at −24°C until used. Subsequently, gDNAs of each fungal isolate were amplified by polymerase chain reaction (PCR) using the universal primers ITS1 (5′-TCCGTAGGTGAACCTGCGG-3′) and ITS4 (5′-TCCTCCGCTTATTGATATGC-3′), following standard protocols (White et al., 1990). All obtained amplicons were sequenced by BMR Genomics s.r.l. (Padua, Italy) and the sequences were compared to those present in GenBank (NCBI) using the basic local alignment search tool (BLAST).

2.5 | Antagonistic assay

The antagonistic microorganisms used in this study were *Beauveria bassiana* and *Bacillus amyloliquefaciens*

belonging to the microbial collection of the phytopathology laboratory of the School of Agricultural, Food, Forestry and Environmental Sciences (SAFE), University of Basilicata (Potenza, Italy). Their antagonistic effect against the most three frequently fungal isolates from kiwifruit KVDS-symptomatic roots was investigated following the contact-phase method (Camele et al., 2019). In particular, 10 µL of *B. amyloliquefaciens* suspension at 10^8 CFU mL^{-1} or small mass from fresh culture (96 h) of *B. bassiana* were deposited singularly in Petri dishes containing PDA nutrient medium on the counter-side to each tested fungus. Three PDA plates inoculated only with each tested fungi without antagonistic microorganisms were used as a negative control. All plates were incubated at 24°C for 3–6 days. The antagonistic effects were evaluated by measuring the diameter of fungal mycelium growth of the three tested fungal species, and the growth inhibition percentage (GIP) was calculated according to Zygadlo et al. (2011):

$$\text{GIP}\,(\%) = \frac{(\text{Gc} - \text{Gt})}{\text{Gc}} \times 100, \quad (3)$$

where Gc is the average diameter of the fungus colony grown on control PDA plates, and Gt is the average diameter of the fungus colony grown on PDA pre-inoculated singularly with each antagonistic microorganism.

2.6 | Plant physiological status

The orchard portion sustainably managed (SUST block) was analysed with a scoring system to determine the evolution (or decline) of the plant physiological status during the trial. Plant (both females and males) were visually classified into one of four categories, depending on the KVDS symptoms on leaves, number and vigour of new shoots and general health status: (a) healthy plants (green); (b) average plants, with medium canopy vigour, new but weak shoots (yellow); (c) very compromised plants, with low canopy vigour, no new shoots and KVDS symptoms on leaves (red) and (d) dead plants (blue) (Figure S8).

2.7 | Statistical analysis

The measurements were statistically analysed by one-way ANOVA followed by post hoc Tukey's honest significant difference (HSD) tests, in the SPSS Statistics 28.0.1.0 (IBM, Armonk, NY, US) statistical environment. The number of replicates for each parameter was specified in the previous paragraphs and also reported in table and figure captions.

TABLE 1 Soil redox potential at pH 7 (Eh_{pH7}) and soil macroporosity in control (CTRL) and KVDS plots at different soil depths.

	0–30 cm	30–60 cm	60–90 cm
Eh_{pH7} (mV)			
CTRL	537 ± 25 a	592 ± 10 a	603 ± 16 a
KVDS	519 ± 19 b	562 ± 12 b	601 ± 16 a
Soil macroporosity (%)			
CTRL	12.35 ± 1.78 a	7.40 ± 1.32 a	3.42 ± 0.74 a
KVDS	8.51 ± 1.61 b	4.90 ± 0.86 b	3.78 ± 1.02 a

Note: Each value represents the mean ± standard deviation ($n = 9$ for Eh_{pH7} and $n = 27$ for macroporosity). Different letters indicate significant differences ($p < .05$) after one-way ANOVA followed by Tukey's HSD test.

3 | RESULTS AND DISCUSSION

3.1 | Physicochemical soil analyses and agronomic practices

As KVDS soils are often subjected to phenomena of compaction and loss of macroporosity (Bardi et al., 2020; Smith et al., 1989; Sofo et al., 2022), Eh_{pH7} measurements can provide direct information on optimal growing conditions for kiwifruit plants. The results of Eh_{pH7} obtained (Table 1) represent a range of values as measured in diverse soils, like the Savanna in West Africa (Husson et al., 2021) or the South West France area (Husson et al., 2018). At 0–30 cm, Eh_{pH7} was 537 mV in CTRL soils and 519 mV in KVDS soils, whereas at 30–60 and 60–90 cm, soils were more oxidized in both groups, with higher Eh_{pH7} values (Table 1). Frequently in conservation agriculture, the Eh_{pH7} of the topsoil is lower than that of the deeper horizons, which is attributed to the high input of biomass on the soil surface (Husson et al., 2021). This was likely because of the fact that, even if the deeper horizons were waterlogged and with lower macropores (Table 1), and thus less aerobic and potentially with a lower Eh_{pH7}, they contained lower quantity of organic matter than the topsoil in both CTRL and KVDS groups (Table S1).

The agroecological management of orchards is one way to correct the oxidized soil-plant systems because it involves enriching soils with organic matter to create a stable porosity produced by enzymatic reactions and stabilized by the presence of clay particles (de Andrade Bonetti et al., 2017; Hassink, 1997; Stegarescu et al., 2020). Organic matter in soil acts as a reserve of electrons, and as it is increased the more it corrects oxidized soils, enhancing the microbial biomass content and the overall enzyme activities in amended soils (García-Gil et al., 2000, 2010). A homogeneous stratum richer in organic carbon and electrons can be obtained by bringing large quantities of biomass with cover crop

residue on the ground each year (Rivière et al., 2022). Also, cover crop root biomass impacts the soil structure and anecic earthworms develop, and create stable galleries and macropores (Kavdir & İlay, 2011).

An increase in carbon inputs has a positive impact on the Eh-pH couple (Husson et al., 2016), allowing plants to maintain the microbiota of mycorrhizal and rhizospheric bacteria essential for feeding and protecting themselves. The absence of these microbial populations in KVDS orchards has been recently noted by Manici et al. (2022), as well as the importance of restoring the ideal conditions for their development. We analysed the impact of a large quantity of compost added in 2017 in one kiwifruit orchard susceptible to the KVDS: after three growing seasons (2019), the orchard with 80 t ha^{-1} (ploughed soil), showed a larger number of trees free of KVDS symptoms compared to the orchard that received a larger quantity of compost (130 t ha^{-1}) (Bardi et al., 2020). This positive result supports the need to de-compact soil to create an aerated mechanical structure and supply soils with a significant biomass (in this case compost), for optimal physicochemical parameters.

Our results (Table 1 and Table S1) suggest that a higher clay content (Table S1) and reduced macroporosity contributed to the occurrence of KVDS. The latter was found to be significantly lower in both the 0–30 cm and 30–60 cm layers of KVDS soils (Table 1), where the kiwifruit plant roots are more concentrated.

Root pruning (Figure S2) was performed after we noticed that peripheral roots were mainly affected by KVDS (>70 cm from the plant). Our goal was to allow the new roots to develop in the sustainable managed soil (SUST group) or in the peat substrate (SUST-PE) and evaluate the fungal species colonizing the roots. Root pruning practice was carried out for stimulating the release of new, healthy roots from the cut roots, so facilitating the development and regeneration of the root system after the damage because of KVDS in a changing soil management aimed at regenerating the soil.

3.2 | Soil drainage and piezometers data

Higher water levels were recorded at the beginning of the monitoring with piezometers in February 2021 and showed a decrease after the drainage system instalment. The drainage system reduced the water excess and, over 2 years, increased and improved the undersoil water circulation in the KVDS area. Figure 1b shows the relationship between rain and soil water table, that was higher in 2021 and lower in 2022 and 2023. We observed an increased water table only after abundant rain events, with a positive water outflow that ensured almost 60 to 90 cm of water-free soil. As commented later on, these water dynamics had a good impact on the plant status and on soil health. For a comparison, in the CTRL plot without drainage, the water movement was active (Figure 1a), showing small peaks of water table only after heavy rain events.

3.3 | Root microscopy analysis and morphometric parameters

Microscopy analysis revealed considerable damage to the KVDS roots (Figure 2a,c), with flaking and browning of the rhizodermis (observed macroscopically; Figure S9), rhizodermis poorly visible, parenchyma cells that lost their round shape, cortical area with a clear loss of cellular turgor, decay of the central stele and clear detachment of the cortex from the central stele (Figures S10 and S11). Detachment of tissue layers in kiwifruit roots was observed by Bardi et al. (2020) by scanning electron microscopy analysis. In contrast, the CTRL roots had healthy roots with no tissue breakdown or decomposition (Figure 2b,d). In this case, the rhizodermis was visible, the cortical zone had numerous round cells rich in starch granules and with large intracellular spaces, the endodermis layer was clear and the central stele showed large xylem vessels and evident phloem with prominent nuclei.

PAS-emallume staining of KVDS roots, colouring mostly starch and cellulose, confirmed the results of safranin-fast green and allowed to highlight other details of the roots (Figure 3a,c), such as starch granules both at the cortex and endodermis level and in the central stele (Figure 3d). Probably, the excessive water present in the compacted soil was not absorbed by the roots because of the non-functionality of the ionic carriers, as a consequence of the low respiratory process and soil hypoxia (Bailey-Serres & Voesenek, 2008; Jackson & Drew, 1984). In these conditions, there is not enough ATP for water transport and the starch is not completely hydrolysed, appearing as granules (Figure 3d). On the other hand, in CTRL roots, starch granules at the cortex and central stele level were scarce (Figure 3c), as the reserve starch, under well oxygenated, aerobic conditions, is consumed (respired). In this case, the energy can be used to activate the ion pumps, so the roots do not undergo water stress.

KVDS roots showed significantly higher values of central stele diameter and area (Table 2), demonstrating the swelling of the damaged roots because of the loss of turgor of the central stele and its detachment from the cortex (Figure S10). By contrary, cortex thickness in the two groups remained constant, so the significant increase in root diameter observed in KVDS roots was mainly caused

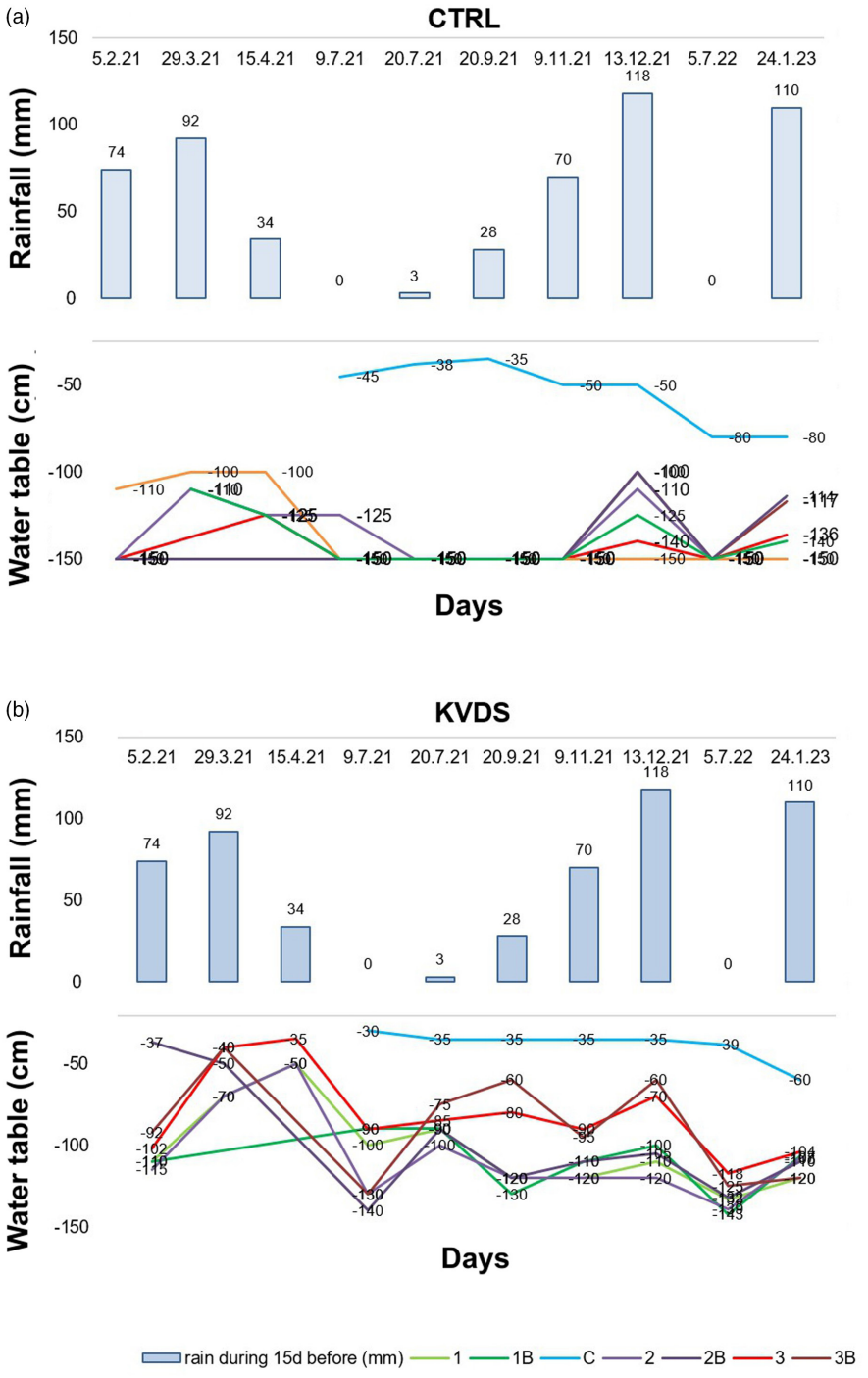

FIGURE 1 Rainfall (blue columns) and water table (lines) measured by the single piezometers (1, 1B, 2, 2B, 3, 3B and C) described in the materials and methods section in (a) control (CTRL) and (b) sustainably managed (SUST) blocks of the orchard. Single values for each data point are shown.

by the variations of central stele size, as shown by the significantly higher ratio of central stele area/cortex area (Table 2). The rhizodermis thickness in CTRL roots was 48.8 μm and the average area of the parenchymatic cells was 1980.3 μm^2, whereas the respective values in KVDS roots were 17.0 μm and 1204.1 μm^2 respectively (Table 2).

The root characteristics observed in KVDS plants (Figures 2 and 3; Figures S9–S11) were probably induced by excess water in the soil. Indeed, water stagnation and decreased oxygen around the roots (soil hypoxia conditions) have a negative, rapid and significant effect on the physiological state and growth of kiwifruit plants, whose roots have a high oxygen consumption but very limited intercellular spaces (Smith et al., 1989). For this reason, the species is considered highly sensitive to hypoxic soil conditions (Jackson & Drew, 1984). Low oxygen concentration could also induce the loss of cortical tissue stiffness observed in the roots of KVDS-affected plants because of the induction of certain hydrolytic enzymes (Bailey-Serres & Voesenek, 2008).

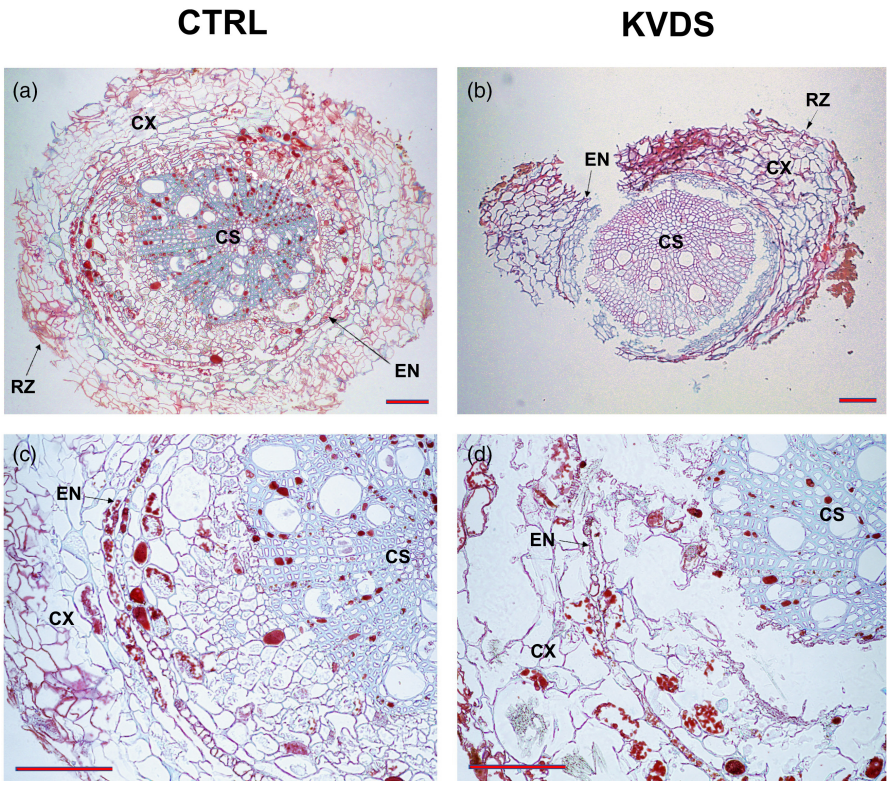

FIGURE 2 Cross sections of (a, c) control (CTRL) and (b, d) KVDS-symptomatic roots (KVDS). Staining with safranin-fast green. CS, central stele; CX, cortex; EN, endodermis; RZ, rhizodermis. Bars = 200 μm.

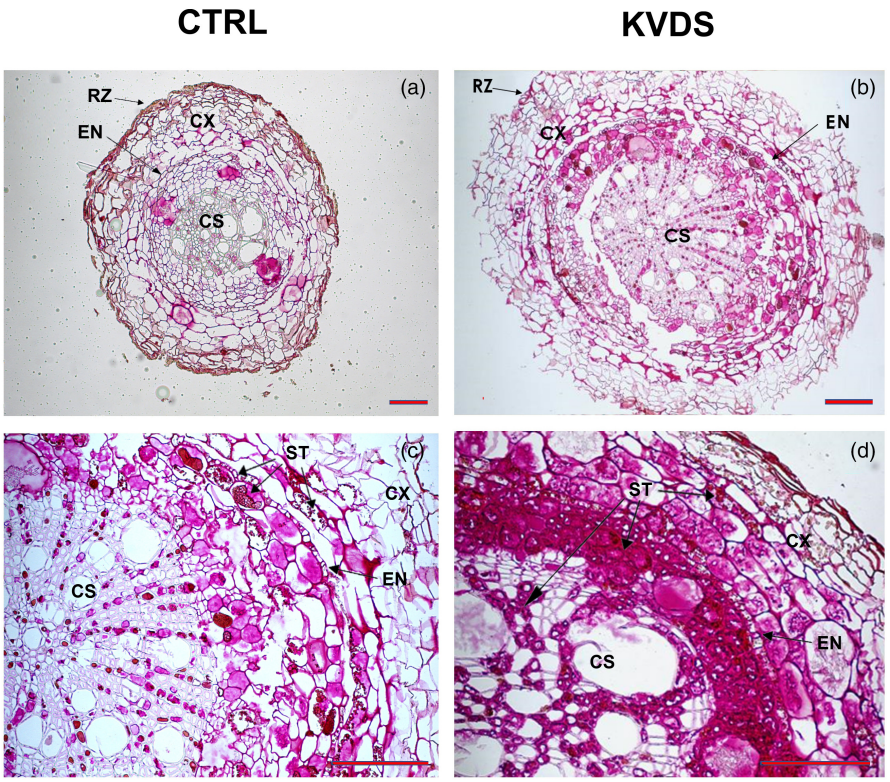

FIGURE 3 Cross sections of (a, c) control (CTRL) and (b, d) KVDS-symptomatic roots (KVDS). Staining with PAS-emallume. CS, central stele; CX, cortex; EN, endodermis; RZ, rhizodermis; ST, starch granules. Bars = 200 μm.

3.4 | Identification of potential pathogenic fungi and biocontrol antagonists

A total of 10 different fungal species were isolated from root samples of the four groups of plants (CTRL, KVDS, SUST and SUST-PE), identified either morphologically and molecularly, and their frequency of isolation is calculated and listed in Table 3. Among the fungal isolates, *Paraphaeosphaeria michotii*, *Ilyonectria vredenhoekensis* and *Fusarium oxysporum* were isolated more frequently,

TABLE 2 Root morphometric parameters in control (CTRL) and KVDS-symptomatic plants.

	Root diameter (mm)	Total root area (mm^2)	Rhizodermis thickness (μm)	Parenchymatic cell area ($μm^2$)	Cortex thickness (mm)	Cortex area (mm^2)	Central stele diameter (mm)	Central stele area (mm^2)	Central stele area/cortex area
CTRL	1.169 ± 0.131 b	1.073 ± 0.254 b	48.8 ± 5.9 a	1980.3 ± 195.3 a	0.197 ± 0.021 a	0.575 ± 0.033 b	0.726 ± 0.080 b	0.415 ± 0.072 b	0.72 ± 0.07 b
KVDS	1.426 ± 0.059 a	1.643 ± 0.177 a	17.0 ± 3.5 b	1204.1 ± 352.6 b	0.202 ± 0.032 a	0.772 ± 0.056 a	1.006 ± 0.057 a	0.838 ± 0.085 a	1.03 ± 0.08 a

Note: Each value represents the mean ± standard deviation ($n = 60$). Different letters indicate significant differences ($p < .05$) within columns after one-way ANOVA followed by Tukey's HSD test.

with frequencies of 28.6, 21.4 and 14.3%, respectively, from KVDS roots. The same three fungal species were isolated from SUST roots with a frequency of 22.2, 11.1 and 20.6% respectively. The SUST-PE group showed reduced values of the isolation frequency for the three fungal species of 13.4, 4.5 and 6.6% respectively. None of the three dominant fungal species were isolated from CTRL roots (Table 3).

Some other fungal species, such as *Phytophtora* spp., *Phytopythium* spp. and *Desarmillaria tabescens*, were also isolated and reported as potential causes of the KVDS [1,5,12], although the pathogenicity tests in those studies were conducted in potted young plants under controlled conditions, where the potential pathogenicity of the pathogenic microorganisms was fully expressed without other microbial competitors, and the plants were relatively weak. Other fungal species, including *Phytophtora* spp., *Phytopythium* spp. and *Desarmillaria tabescens*, were also isolated and reported as potential causes of the KVDS. Finally, *Dactylonectria macrodidyma* and *Thielaviopsis basicola* were also proposed as other KVDS-related pathogens (Savian et al., 2022).

In this scenario, KVDS could be defined as a soil dysbiosis-driven physiopathy. Indeed, substantial differences in fungal and oomycete community structure were observed between healthy and KVDS-symptomatic kiwifruit vines. Furthermore, the relationships between fungi and bacteria could play a key role. Interestingly, Spigaglia et al. (2020) tried to find a correlation between the hypoxic and waterlogged soil conditions, highlighted by Sofo et al. (Sofo et al., 2022) and Savian, Ginaldi, et al. (2020) as possible co-factors of KVDS, and anaerobic bacteria belonging to *Clostridium* spp. Also, in this case, it is not certain if these potentially pathogenic bacteria are cause or consequences of the KVDS, while they could be related to hypoxic soil conditions (Bardi, 2020). Indeed, the authors concluded that 'The occurrence of anaerobic bacteria does not exclude the possibility that other microorganisms could play additional/synergic role(s) in causing the kiwifruit vine decline'. Furthermore, for investigating the probable causes of KVDS, Savian, Ginaldi, et al. (2020) used transmission electron microscope for studying root ultrastructures of artificially flooded plants grown in a controlled environment, finding no pathogen-related structures (hyphae, conidia) in the xylem nor pathogen-related symptoms (such as xylem cell wall deterioration). This would, however, not exclude the role of some pathogenic microorganisms. The absence of beneficial biocontrol and/or plant-growth-promoting bacteria in overexploited soils of kiwifruit orchards is also considered a possible driver of KVDS (Manici et al., 2022).

The in vitro screening of antagonistic activity (Figure 4) suggests that both the antagonist

	Number (*n*) and frequency (%) of fungal taxa			
	CTRL	KVDS	SUST	SUST-PE
Fusarium oxysporum	—	12 (14.3)	13 (20.6)	3 (6.6)
Fusarium spp.	—	10 (11.9)	18 (28.6)	2 (4.5)
Paraphaeosphaeria michotii	—	24 (28.6)	14 (22.2)	6 (13.4)
Ilyonectria vredenhoekensis	—	18 (21.4)	7 (11.1)	2 (4.5)
Penicillium spp.	3 (5.4)	—		8 (17.7)
Trichoderma spp.	13 (23.2)	—	6 (9.5)	18 (40.1)
Machrophomina phaseolina		17 (20.2)		
Phytophthora cinnamomi	17 (30.4)			
Cladosporium spp.	12 (21.4)			
Pythium spp.	9 (16.1)		1 (1.6)	3 (6.6)
Others	2 (3.5)	3 (3.6)	4 (6.4)	3 (6.6)
Total samples	56 (100)	84 (100)	63 (100)	45 (100)

TABLE 3 Number (and frequency in brackets) of the fungal taxa isolated from symptomatic kiwifruit roots. The percentages less than 5% were not considered and grouped as 'others' ($n = 56$, 84, 63 and 45, for CTRL, KVDS, SUST and SUST-PE groups respectively).

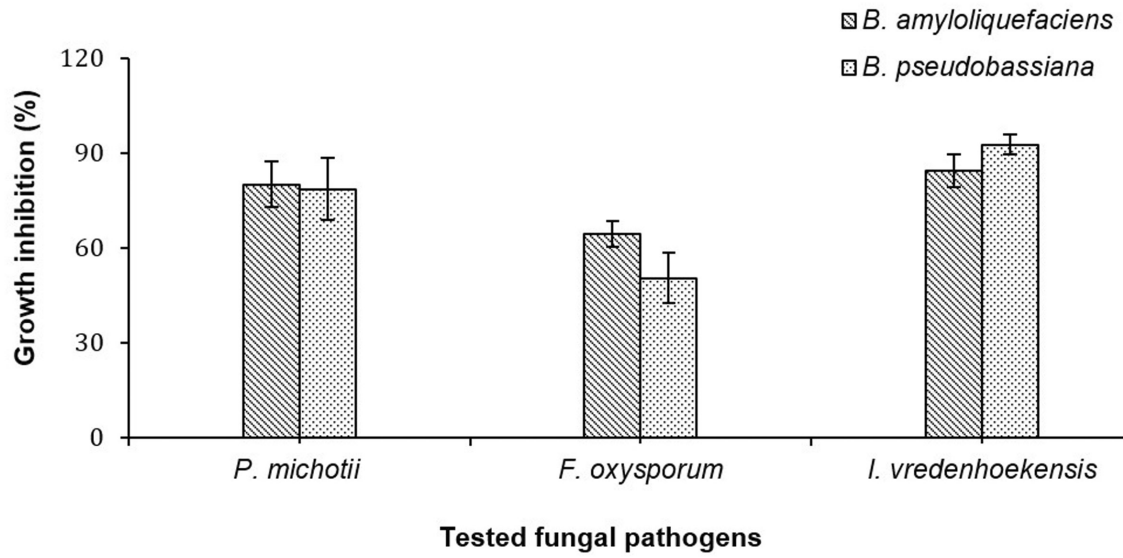

	B. amyloliquefaciens	*B. pseudobassiana*
P. michotii	+++	+++
F. oxysporum	++	++
I. vredenhoekensis	+++	++++

FIGURE 4 Antagonistic activity of two tested micro-organisms against three fungi isolated from kiwifruit roots. ++ moderate activity; +++ high activity; ++++ very high activity. Each column represents the mean ± standard deviation ($n = 10$). Different letters indicate significant differences after one-way ANOVA followed by Tukey's HSD test.

microorganisms had a higher contrasting effect against *I. vredenhoekensis* and *P. michotii*, whereas only a moderate effect was observed against *F. oxysporum*. The highest antagonistic effect was observed in the case of *B. bassiana* against *I. vredenhoekensis* with a growth inhibition percentage of 92.6% (Figure 4).

TABLE 4 Scoring table of the physiological status of kiwifruit plants during the experimental trial in the sustainable-managed block (SUST) of the kiwifruit orchard.

Scoring	2021 (%)	2022 (%)	2021–2022 (difference %)	2023 (%)	2022–2023 (difference %)
Green	30.1	68.6	38.5	76.2	7.6
Yellow	56.3	26.5	−29.8	19.8	−6.7
Red	12.6	4.9	−7.7	4.0	−0.9
Blue	1.0	0.0	−1.0	0.0	0.0
Male green	91.3	83.3	−8.0	80.0	−3.3
Male yellow	4.3	12.5	8.2	12.0	−0.5
Male red	0.0	0.0	0.0	4.0	4.0
Male blue	4.3	4.3	0.0	4.3	0.0

Note: Plant classification: (a) healthy plants (green); (b) average plants, with medium canopy vigour, new but weak shoots (yellow); (c) very compromised plants, with low canopy vigour, no new shoots and KVDS symptoms on leaves (red); (d) dead plants (blue).

3.5 | Plant physiological status

The plant status scoring (Table 4) in the time showed good and fast canopy recovery during the first year (2021–2022), with a constant but slower recovery during the second year (2022–2023), probably because of the very warm and dry condition of the 2022 summer period. In the SUST block, the severity of KVDS symptoms decreased over the time, indicating the importance of the interventions carried out in reducing syndrome severity and counteracting its emergence. The frequency of plants classified as green increased considerably in 2022 (+38.5%), while the number of plants classified as yellow and red decreased (−29.8% and −7.7% respectively). The positive trend continued in 2023, even if at a smaller scale, likely because of the warm 2022 summer that had a negative higher impact on the canopy status.

4 | CONCLUSIONS

The adoption of sustainable agronomic practices, such as the application of precision irrigation, the addition of organic matter after the emergence of KVDS symptoms, the installation of a drainage system and the decompaction of soil by adequate cover crops, created favourable growth conditions for kiwifruit plants, whose physiological status ameliorated. The results also indicate that different fungal species, including a few pathogenic ones (*P. michotii*, *F. oxysporum* and *I. vredenhoekensis*), were associated with KVDS. Their role could not be attributed as the reason for the kiwifruit decline but consequential (after root decay) and eventually favoured by waterlogging conditions, soil compaction and poor soil aeration leading to root decline. A promising antimicrobial effect by two antagonist microorganisms was observed, which could be used as biocontrol agents against the most dominant potentially fungal pathogens associated with KVDS.

We demonstrated that the amelioration of soil chemico-physical status by the adoption of a sustainable agroecosystem management improved the physiological conditions of KVDS-symptomatic kiwifruit vines and protected them against potential fungal pathogens. The sustainable agronomic practices implemented in this study are applicable in most kiwifruit growing regions, excepting root pruning being used in severe situations, once the vines have been lost to KVDS and might otherwise be pulled out and replaced. A sustainable and agroecological approach to kiwifruit orchard management represents a technically feasible solution to halt the spread of KVDS by recreating the natural environmental conditions where kiwifruit plants thrive.

ACKNOWLEDGEMENTS

This work was supported by the Zespri lnnovation project 'Water and Soil Management of Gold3 Kiwifruit in ltaly' (project number GI21020). We are grateful to the owner of the experimental field Gianni Zoppellaro and to the agronomist Fabio Marocchi for their support during field activities. We thank Dr. Angelo Tuzio, Dr. Domenico Laterza and Dr. Roberto Di Biase for their technical support.

CONFLICT OF INTEREST STATEMENT

The authors declare that they have no known competing financial interests or personal relationships that could have appeared to influence the work reported in this paper.

DATA AVAILABILITY STATEMENT

Data will be made available on request.

ORCID

Adriano Sofo https://orcid.org/0000-0003-0305-308X

REFERENCES

Albrecht, G., & Mustroph, A. (2003). Localization of sucrose synthase in wheat roots: Increased *in situ* activity of sucrose synthase correlates with cell wall thickening by cellulose deposition under hypoxia. *Planta*, *217*, 252–260. https://doi.org/10.1007/S00425-003-0995-6/TABLES/2

Bailey-Serres, J., & Voesenek, L. A. C. J. (2008). Flooding stress: Acclimations and genetic diversity. *Annual Review of Plant Biology*, *59*, 313–339. https://doi.org/10.1146/ANNUREV.ARPLANT.59.032607.092752

Bardi, L. (2020). Early kiwifruit decline: A soil-borne disease syndrome or a climate change effect on plant–soil relations? *Frontiers in Agronomy*, *2*, 3. https://doi.org/10.3389/FAGRO.2020.00003/BIBTEX

Bardi, L., Nari, L., Morone, C., Faga, M. G., & Malusà, E. (2020). Possible role of high temperature and soil biological fertility on kiwifruit early decline syndrome. *Frontiers in Agronomy*, *2*, 13. https://doi.org/10.3389/FAGRO.2020.580659/BIBTEX

Camele, I., Elshafie, H. S., Caputo, L., Sakr, S. H., & De Feo, V. (2019). *Bacillus mojavensis*: Biofilm formation and biochemical investigation of its bioactive metabolites. *Journal of Biological Research – Bollettino della Società Italiana di Biologia Sperimentale*, *92*, 39–45. https://doi.org/10.4081/jbr.2019.8296

de Andrade Bonetti, J., Anghinoni, I., de Moraes, M. T., & Fink, J. R. (2017). Resilience of soils with different texture, mineralogy and organic matter under long-term conservation systems. *Soil and Tillage Research*, *174*, 104–112. https://doi.org/10.1016/J.STILL.2017.06.008

Donati, I., Buriani, G., Cellini, A., Mauri, S., Costa, G., & Spinelli, F. (2014). New insights on the bacterial canker of kiwifruit (*Pseudomonas syringae* pv. actinidiae). *Journal of Berry Research*, *4*, 53–67. https://doi.org/10.3233/JBR-140073

Donati, I., Cellini, A., Sangiorgio, D., Caldera, E., Sorrenti, G., & Spinelli, F. (2020). Pathogens associated to kiwifruit vine decline in Italy. *Agriculture*, *10*, 119. https://doi.org/10.3390/AGRICULTURE10040119

García-Gil, J. C., Haller, I., Soler-rovira, P., & Polo, A. (2010). *Effects of conventional and no-tillage soil management and compost and sludge amendment on soil CO_2 fluxes and microbial activities*. Geophysical Research Abstracts.

García-Gil, J. C., Plaza, C., Soler-Rovira, P., & Polo, A. (2000). Long-term effects of municipal solid waste compost application on soil enzyme activities and microbial biomass. *Soil Biology and Biochemistry*, *32*, 1907–1913. https://doi.org/10.1016/S0038-0717(00)00165-6

Hassink, J. (1997). The capacity of soils to preserve organic C and N by their association with clay and silt particles. *Plant and Soil*, *191*, 77–87. https://doi.org/10.1023/A:1004213929699/METRICS

Husson, O., Brunet, A., Babre, D., Charpentier, H., Durand, M., & Sarthou, J. P. (2018). Conservation Agriculture systems alter the electrical characteristics (Eh, pH and EC) of four soil types in France. *Soil and Tillage Research*, *176*, 57–68. https://doi.org/10.1016/J.STILL.2017.11.005

Husson, O., Husson, B., Brunet, A., Babre, D., Alary, K., Sarthou, J. P., Charpentier, H., Durand, M., Benada, J., & Henry, M. (2016). Practical improvements in soil redox potential (Eh) measurement for characterisation of soil properties. Application for comparison of conventional and conservation agriculture cropping systems. *Analytica Chimica Acta*, *906*, 98–109. https://doi.org/10.1016/J.ACA.2015.11.052

Husson, O., Sarthou, J. P., Bousset, L., Ratnadass, A., Schmidt, H. P., Kempf, J., Husson, B., Tingry, S., Aubertot, J. N., Deguine, J. P., Goebel, F. R., & Lamichhane, J. R. (2021). Soil and plant health in relation to dynamic sustainment of Eh and pH homeostasis: A review. *Plant and Soil*, *466*, 391–447. https://doi.org/10.1007/S11104-021-05047-Z

Jackson, M. B., & Drew, M. C. (1984). Chapter 3 – Effects of flooding on growth and metabolism of herbaceous plants. In B. G. Luisa (Ed.), *Flooding and plant growth* (pp. 47–128). Academic Press.

Kavdir, Y., & İlay, R. (2011). Earthworms and soil structure. In A. Karaca (Ed.), *Biology of earthworms* (pp. 39–50). Springer-Verlag.

Ma, Y., Sawhney, V. K., & Steeves, T. A. (2011). Staining of paraffin-embedded plant material in safranin and fast green without prior removal of the paraffin. *Canadian Journal of Botany*, *71*, 996–999. https://doi.org/10.1139/B93-114

Manici, L. M., Saccà, M. L., Scotti, C., & Caputo, F. (2022). Quantitative reduction of soil bacteria and qualitative microbial changes: Biotic components associated to kiwifruit decline. *Plant and Soil*, *477*, 613–628. https://doi.org/10.1007/S11104-022-05470-W/FIGURES/7

Mininni, A. N., Laterza, D., Tuzio, A. C., Di Biase, R., & Dichio, B. (2022). Soil water content monitoring as a tool for sustainable irrigation strategy in a kiwifruit orchard under semi-arid conditions. *Acta Horticulturae*, *1332*, 203–210.

Pansu, M., & Gautheyrou, J. (2006). *Handbook of soil analysis: Mineralogical, organic and inorganic methods*. Springer.

Reid, J. B., Tate, K. G., Brown, N. S., & Cheah, L. H. (1991). Effects of flooding and alluvium deposition on kiwifruit (*Actinidia deliciosa*): 1. Early vine decline. *New Zealand Journal of Crop and Horticultural Science*, *19*, 247–257. https://doi.org/10.1080/01140671.1991.10421808

Rivière, C., Béthinger, A., & Bergez, J. E. (2022). The effects of cover crops on multiple environmental sustainability indicators—a review. *Agronomy*, *12*, 2011. https://doi.org/10.3390/AGRONOMY12092011

Savian, F., Ginaldi, F., Musetti, R., Sandrin, N., Tarquini, G., Pagliari, L., Firrao, G., Martini, M., & Ermacora, P. (2020). Studies on the aetiology of kiwifruit decline: Interaction between soil-borne pathogens and waterlogging. *Plant and Soil*, *456*, 113–128. https://doi.org/10.1007/S11104-020-04671-5/FIGURES/7

Savian, F., Marroni, F., Ermacora, P., Firrao, G., & Martini, M. (2022). A metabarcoding approach to investigate fungal and oomycete communities associated with kiwifruit vine decline syndrome in Italy. *Phytobiomes Journal*, *6*, 290–304. https://doi.org/10.1094/PBIOMES-03-22-0019-R

Savian, F., Martini, M., Ermacora, P., Paulus, S., & Mahlein, A. K. (2020). Prediction of the kiwifruit decline syndrome in diseased orchards by remote sensing. *Remote Sensing*, *12*, 2194. https://doi.org/10.3390/RS12142194

Savian, F., Prencipe, S., Filippini, N., Nari, L., Martini, M., Ermacora, P., & Spadaro, D. (2021). Pathogenicity of *Phytopythium chamaehyphon*: A new player in kiwifruit vine decline syndrome of *Actinidia chinensis* var. deliciosa "Hayward" in Italy. *Plant Disease*, *105*, 2781–2784. https://doi.org/10.1094/PDIS-01-21-0143-SC

Smith, G. S., Buwalda, J. G., Green, T. G. A., & Clarck, C. J. (1989). Effect of oxygen supply and temperature at the root on the

physiology of kiwifruit vines. *The New Phytologist*, *113*, 431–437. https://doi.org/10.1111/J.1469-8137.1989.TB00354.X

Sofo, A., Mininni, A. N., Dichio, B., Mastroleo, M., & Xylogiannis, E. (2022). Physical structure and chemical quality of waterlogged soils in an Italian kiwifruit orchard. *Acta Horticulturae*, *1332*, 195–201. https://doi.org/10.17660/ACTAHORTIC.2022.1332.26

Sotta, N., & Fujiwara, T. (2017). Preparing thin cross sections of *Arabidopsis* roots without embedding. *BioTechniques*, *63*, 281–283. https://doi.org/10.2144/000114621

Spigaglia, P., Barbanti, F., Marocchi, F., Mastroleo, M., Baretta, M., Ferrante, P., Caboni, E., Lucioli, S., & Scortichini, M. (2020). *Clostridium bifermentans* and *C. subterminale* are associated with kiwifruit vine decline, known as moria, in Italy. *Plant Pathology*, *69*, 765–774. https://doi.org/10.1111/PPA.13161

Stegarescu, G., Escuer-Gatius, J., Soosaar, K., Kauer, K., Tõnutare, T., Astover, A., & Reintam, E. (2020). Effect of crop residue decomposition on soil aggregate stability. *Agriculture*, *10*, 527. https://doi.org/10.3390/AGRICULTURE10110527

White, T. J., Bruns, T., Lee, S., & Taylor, J. (1990). Amplification and direct sequencing of fungal ribosomal RNA genes for phylogenetics. *PCR Protocols*, 315–322. https://doi.org/10.1016/B978-0-12-372180-8.50042-1

Zygadlo, J. A., Guzman, C. A., & Grosso, N. R. (2011). Antifungal properties of the leaf oils of *Tagetes minuta* L. and *T. filifolia* Lag. *Journal of Essential Oil Research*, *6*, 617–621. https://doi.org/10.1080/10412905.1994.9699353

SUPPORTING INFORMATION

Additional supporting information can be found online in the Supporting Information section at the end of this article.

How to cite this article: Sofo, A., Dichio, B., Elshafie, H. S., Camele, I., Calabritto, M., Tomasi, I., Mastroleo, M., Xylogiannis, E., D'Ippolito, I., & Mininni, A. N. (2024). Enhancing soil properties through sustainable agronomic practices reduced the occurrence of kiwifruit vine decline syndrome. *Soil Use and Management*, *40*, e13052. https://doi.org/10.1111/sum.13052

Supplementary material

Supplementary Table S1. Soil physicochemical parameters measured at the beginning of the experiment in February 2021 at a depth of 0-30 cm and 30-60 cm in the KVDS and CTRL plots. Each value is the average of three replicates (n = 9).

	KVDS		CTRL	
	0-30 cm	30-60 cm	0-30 cm	30-60 cm
pH	7.4	7.3	6.9	6.7
Electrical conductivity (mS cm^{-1})	0.242	0.148	0.505	0.371
Organic matter (%)	3.39	2.60	3.07	2.85
Total limestone	traces	traces	traces	traces
Skeleton	traces	absent	traces	absent
Soil texture				
Sand (2.0 – 0.020 mm) (%)	25	24	33	29
Silt (0.020 – 0.002 mm) (%)	32	32	29	32
Clay (< 0.002 mm) (%)	43	44	39	40
Soil texture	clay	clay	clay	clay
Nutrients				
N total (%)	0.195	0.153	0.180	0.161
P absorbable (ppm)	41	22	37	31
Fe absorbable (ppm)	15.8	17.2	35.5	40.0
Mn absorbable (ppm)	28.1	27.6	56.1	65.9
Cu absorbable (ppm)	4.2	2.7	3.9	3.7
Zn absorbable (ppm)	3.0	0.8	4.3	4.0
Ca exchangeable (ppm)	4,133	3,900	4,353	4,920
Mg exchangeable (ppm)	600	567	480	493
K exchangeable (ppm)	134	96	203	143
Na exchangeable (ppm)	87	80	100	95
Cation exchange capacity				
Cation exchange capacity (meq 100 g soil^{-1})	26.39	24.82	27.03	30.49
Ca (meq 100 g soil^{-1})	20.67	19.50	21.77	24.61
Mg (meq 100 g soil^{-1})	5.00	4.72	4.00	4.10
K (meq 100 g soil^{-1})	0.34	0.25	0.52	0.36
Na (meq 100 g soil^{-1})	0.38	0.35	0.43	0.42
Base saturation (%)	100	100	98.9	96.5

Supplementary Table S2. Composition of the applied cover crops.

Species	Variety	Weight (%)
Avena strigosa	Iapar	40
Raphanus sativus	Cassius	30
Eruca vesicaria	Rocket	10
Sinapis alba	Rumba	10
Brassica juncea	Terminator	10

Supplementary Table S3. Chemical parameters of the applied manure.

pH	8.4
Salinity (mS cm^{-1})	2.6
Water (%)	48.27
Residue at 100 °C (%)	51.73
Total N (% dry)	2.61
Organic N (% dry of total N)	99.23
Organic C (% dry)	36.54
Humic and fulvic C (%)	9.0
C/N	16,378.2
P_2O_5 (mg kg^{-1} dry)	11,254.492
K (mg kg^{-1} dry)	354.130
Al (mg kg^{-1} dry)	< 0.001
Sb (mg kg^{-1} dry)	1.786
As (mg kg^{-1} dry)	0.036
Cd (mg kg^{-1} dry)	4,133
Cr (mg kg^{-1} dry)	48.507
Cr^{+6} (mg kg^{-1} dry)	0.184
Hg (mg kg^{-1} dry)	< 0.001
Mo (mg kg^{-1} dry)	< 0.001
Ni (mg kg^{-1} dry)	< 0.001
Pb (mg kg^{-1} dry)	62.196
Cu (mg kg^{-1} dry)	58.327
Sn (mg kg^{-1} dry)	16.367
Zn (mg kg^{-1} dry)	118.143

Supplementary Figure S1. (above and center) Kiwifruit vines showing severe visual symptoms of KVDS; (below) Map of the KVDS and CTRL blocks in the experimental orchard.

.

Supplementary Figure S2. Excavation showing kiwifruit roots (left) before root pruning and (right) after root pruning.

Supplementary Figure S3. (above) Cover crops in the soils with root-pruned plants (March 2022); (below) the soil-decompacting crop *Raphanus sativus*.

Supplementary Figure S4. Excavations for the setting-up of the water drainage plant.

Supplementary Figure S5. Piezometers placed in the field.

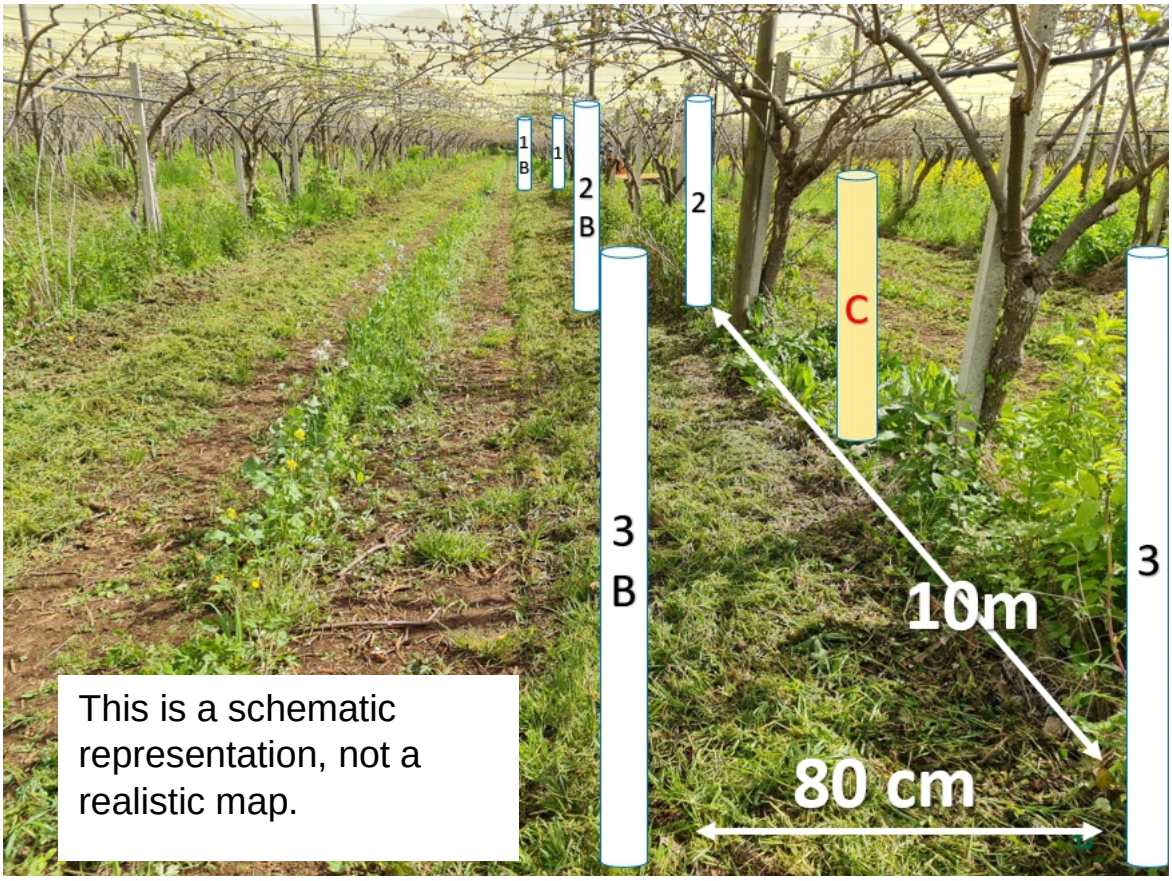

Supplementary Figure S6. Soil macroporosity measured at depths of 0-30 (upper row) and 30-60 cm (lower row) in control soil (CTRL, left) and in soils with KVDS-symptomatic plants (KVDS, right). Bars = 1 mm.

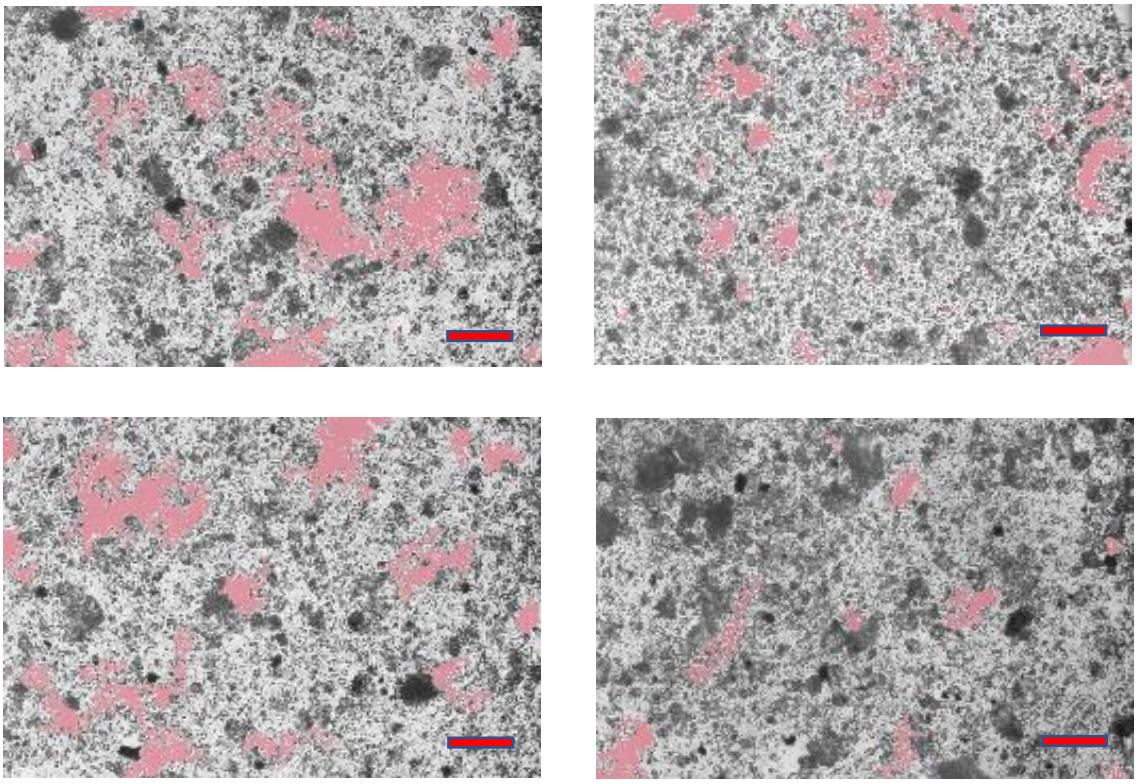

Supplementary Figure S7. Excavation of trenches in the inter-row area for root sampling (February 2022).

Supplementary Figure S8. Scoring map of the general physiological status of kiwifruit plants in the RP block in 2021, 2022 and 2023. Plant classification: a) healthy plants (green); b) average plants, with medium canopy vigor, new but weak shoots (yellow); c) very compromised plants, with low canopy vigor, no new shoots and KVDS symptoms on leaves (red); d) dead plants (blue).

	Map legend
G	Green
Y	Yellow
R	Red
D	Blue
MG	Male green
MY	Male yellow
MR	Male red
MD	Male blue

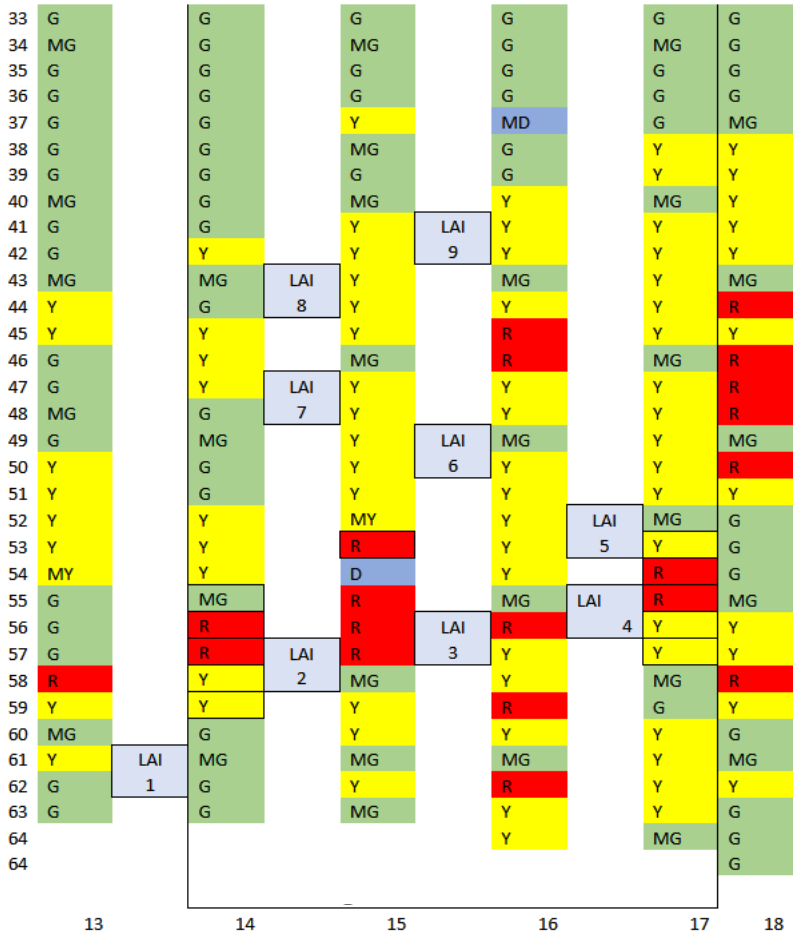

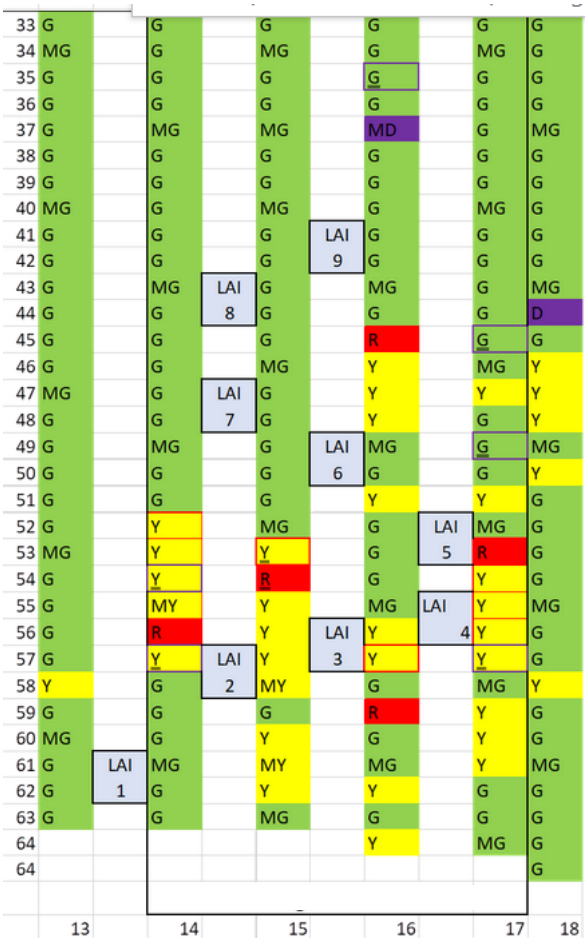
LAI 1
LAI 2
LAI 3
LAI 4
LAI 5
LAI 6
LAI 7
LAI 8
LAI 9
13
14
15
16
17
18

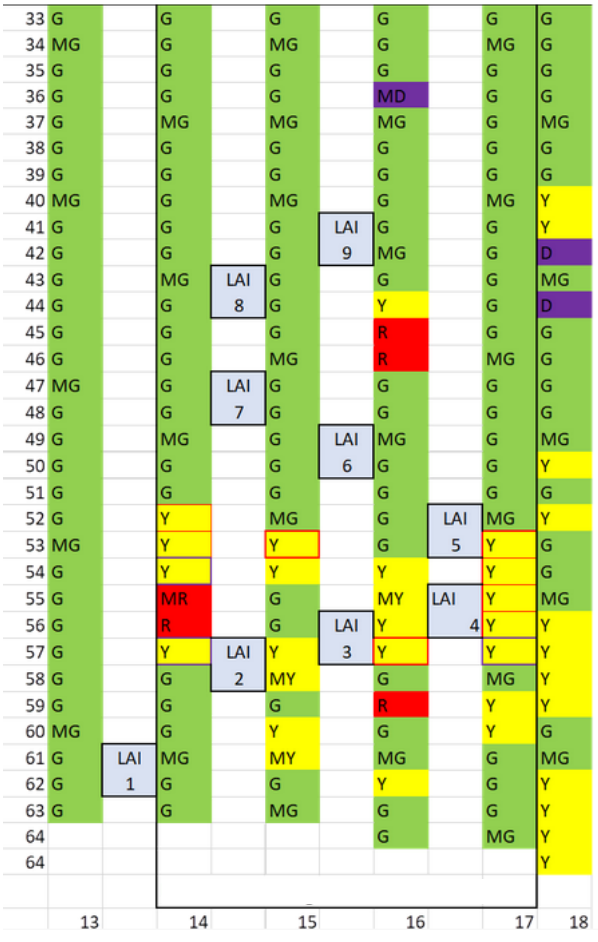
LAI 1
LAI 2
LAI 3
LAI 4
LAI 5
LAI 6
LAI 7
LAI 8
LAI 9
13
14
15
16
17
18

Supplementary Figure S9. Rhizodermis in control (CTRL, above) and KVDS-symptomatic roots (KVDS, below). Photo taken with a stereomicroscope Bresser Optik Science ETD 101 (Bresser GmbH, Rhede, Germany). Bars = 100 µm.

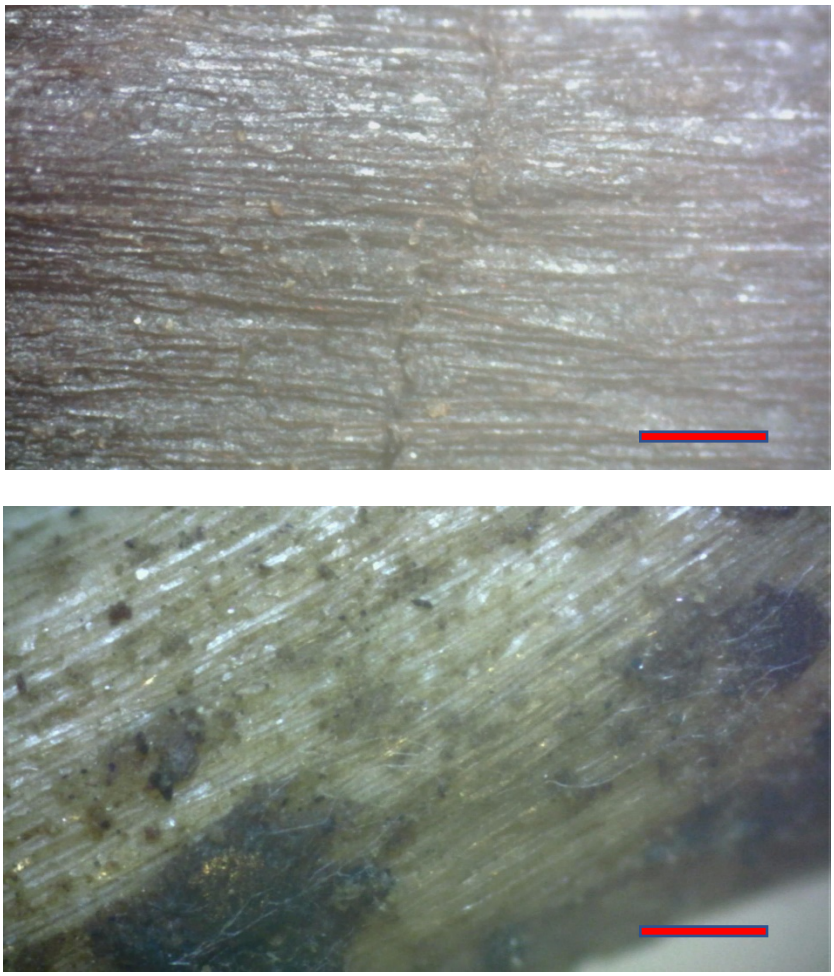

Supplementary Figure S10. Detachment of the cortex from the central stele in KVDS-symptomatic roots. Photo taken with a stereomicroscope Bresser Optik Science ETD 101 (Bresser GmbH, Rhede, Germany).

Supplementary Figure S11. Central stele in control (CTRL, above) and KVDS-symptomatic roots (KVDS, below). Photo taken with a stereomicroscope Bresser Optik Science ETD 101 (Bresser GmbH, Rhede, Germany). Bars = 150 µm.